International Journal of Advanced Technology and Engineering Exploration, Vol 11(120)
ISSN (Print): 2394-5443 ISSN (Online): 2394-7454
http://dx.doi.org/10.19101/IJATEE.2024.111100971

Research Article

Developmental study of a 3D prosthetic foot using finite element analysis

Noor B. Mohammed and Yassr Y. Kahtan*
Department of Prosthetics and Orthotics Engineering, College of Engineering, Al-Nahrain University, Baghdad, Iraq

Received: 05-June-2024; Revised: 24-November-2024; Accepted: 26-November-2024

Abstract
The most popular type of prosthetic foot is the energy storage and return (ESAR) foot, which provides stability and balance during gait. The study focuses on the development of an ESAR prosthetic foot using various types of acrylonitrile butadiene styrene (ABS) material. The primary aim was to enhance stability and balance during gait. Two strategies were implemented: modifying the material to improve its mechanical properties and altering the foot design. The findings revealed that design changes were more critical to the model's success than material adjustments. Finite element analysis (FEA) was used to compare the stress responses of ABS, carbon fiber polylactic acid (PLA), and polyethylene terephthalate glycol (PETG) during gait cycles. During the heel strike (HS) phase, stress values were measured as follows: ABS Plus at 11.562 MPa, carbon fiber PLA at 11.723 MPa, and PETG at 1.9806 MPa. Notably, the total deformation was less for carbon fiber PLA and PETG compared to ABS Plus, with values recorded at 1.9671 mm, 1.7445 mm, and 0.55776 mm, respectively. The most successful design iteration (design F) demonstrated optimal results with a total deformation of 4.7254 mm, strain energy of 0.1863 mJ, and von Mises stress of 19.57 MPa, achieving a safety factor of 1.584 overall. Conversely, other designs, particularly design E, exhibited high stress levels (42.816 MPa) and safety factors below the acceptable threshold of 1.5. Dynamic analysis showed poor performance under fatigue testing, with safety factors ranging from 1.0368e-7 to 8.9274e-8 indicating a high risk of structural failure. Overall, the study highlights the critical need for effective design modifications in prosthetic foot development to ensure safety and functionality for amputees.

Keywords
Energy store and return, Finite element analysis, Prosthetic foot, Stress and deformation, Carbon fiber, Gait cycle.

1.Introduction
Prosthetic limbs have been an option to replace amputated limbs for many years. Because it keeps the prosthetic balanced and stable throughout the gait cycle, the foot is the most important component of a prosthesis. Energy storage and return (ESAR) feet are currently the most prevalent kind. It is constructed from components that resemble springs or materials like carbon fiber, which enable mechanical energy to be retained when standing and released during push off (PO) during the gait cycle [1]. This feature improves the gait by lowering mechanical stress. Studies have shown that the PO phase during walking depends on the stored energy, indicating that the use of the ESAR feet, as opposed to conventional rigid feet, is more appropriate to provide this functionality [2].

The price of prosthetic feet is high. The least expensive foot is the stiff heel cushioned ankle (SACH) device, which is intended for people with low energy activity levels [3–4]. A major benefit in the design of good prostheses today is the high ESAR [5]. Despite of the apparent absence of improved walking economy, the majority of patients who use lower limb prostheses still favor ESAR feet. This raises the question whether there ought to be any extra functional advantages beyond economic ones. In the past, the ESAR feet have been shown to reduce mechanical stress, which may assist in preventing overload injuries in natural or prosthetic legs [6]. Alternatively, recent research on the gait of people who have had their lower limbs amputated leads one to hypothesize that the improved ankle PO power of an ESAR foot might improve gait stability and symmetry [7]. In recent years, additive manufacturing (AM), commonly known as three-dimensional (3D) printing, has replaced conventional methods for producing prosthetics [8]. Different 3D

*Author for correspondence

printing technologies, including the laser sintering technique [9–10] and fused deposition modelling (FDM) [11], were used for lower limb prosthetics. Complex shapes that are typically difficult or expensive to manufacture using traditional methods can now be designed using 3D printing [12]. This allows for the creation a that is fitted to the wearer's comfort. The creation of sophisticated 3D printing materials has improved prosthetic properties, making them more lightweight and functional [13]. As science and materials advanced, AM techniques emerged, and, with them, attempts to create 3D printable prostheses that mimicked the features of the ESAR foot surfaced [3]. When designing prosthetic feet for patients, engineers have more creative freedom thanks to 3D printing. After patient testing, computer-aided design (CAD) models can be altered and changed. This process allows for producing prosthetic feet in small quantities at affordable prices or in response to specific customer requests. Plastic filaments made from a variety of materials are available and have good mechanical qualities. Various acrylonitrile butadiene styrene (ABS) and Polycarbonate/acrylonitrile butadiene styrene (PC-ABS) varieties as well as other materials like carbon fiber, polylactic acid (PLA), and polyethylene terephthalate glycol (PETG) are employed. Plastics' capacity to store energy makes them useful during the PO phase of the gait cycle [5].

One of the challenges encountered during the development of a previous design was achieving an ideal prosthetic foot design made from plastic materials capable of withstanding the stresses generated during walking. These stresses arise from both the individual's weight and the forces exerted by the ground on the foot. Additionally, the goal was to create a low-cost design using materials readily available in local markets while ensuring the manufacturing process was simple, time-efficient, and did not involve complex procedures.

This paper aims to build on previous research [14] that dealt with an attempt to manufacture an energy storage foot from ABS material which broke and failed in manufacturing. Therefore, this research attempts to avoid the failure through two methods: the first was attempts to change the materials depending on the most available materials in Iraq and the most distinctive in terms of properties. The second method involved modifying the foot design using the SolidWorks simulation program to facilitate theoretical development. This work highlights the challenges of incorporating 3D printing into the production of prosthetic feet, primarily due to the significant stresses imposed on the foot during walking.

The research is divided into six sections. Section 1 introduces prosthetic feet, while Section 2 reviews prior research in this area. Section 3 provides a comprehensive overview of the theories and techniques employed. The results are presented in Section 4, followed by a discussion of key conclusions and insights in Section 5. Finally, Section 6 covers the conclusion and suggestions for future work.

2.Literature review

A literature review was conducted on the latest research on energy-storing feet to identify the advantages of the work and the latest developments in this field.

Segal et al. [15] investigated the impact of a prototype microprocessor-controlled prosthetic foot on amputee gait, focusing on its ability to store and return energy during the loading and PO phases. Compared to non-amputees, lower limb amputees have a more energetically costly stride, compensations at other joints, and a decreased prosthetic ankle PO due to their absence of functioning ankle muscle. In a random order, unilateral transtibial amputees wore their previously prescribed foot, a conventional foot and the controlled energy storage and return (CESR) prosthetic foot. In comparison to normal and prosthetic limbs, a study evaluating the prosthetic foot with a CESR system discovered that it enhanced energy storage during early stance, peak PO power, and PO labor. But as compared to conventional and prescribed foot, the net metabolic cost for CESR stayed the same, maybe because of its heavier weight, lack of customized size and stiffness, and lack of experience with CESR and conventional foot. The study indicates that more design changes are required to enhance the walking economy of amputees.

Ray et al. [16] examined how lower limb mechanical work profiles changed when walking after three weeks of adjusting to a new prosthesis was the goal of the study. A retrospective examination of 22 patients who had a unilateral transtibial amputation was conducted. After receiving a new prosthesis at their existing degree of mobility (K3 or above), the participants wore it for three weeks. At 0, 1.5, and 3 weeks into the adaptation period, kinematic and kinetic measurements were taken while walking overground at a self-selected rate. A six-degree-of-freedom model for the knee and hip and a unified deformable segment model were used to quantify the positive and negative work performed by the prosthesis and sound ankle-foot. Hamzah and Gatta [17] replicated the movement of a healthy human foot, creating an innovative carbon fiber prosthesis. The material used is a carbon fiber-epoxy composite. The method is based on the design of an ankle prosthesis made of carbon fiber (rolled shape), built-in geometry and modeling of the foot. With AutoCAD, ANSYS was used to model the finite element analysis (FEA) based on the geometry recovered from AutoCAD. The material used in manufacturing is carbon Epoxy fiber composite for a lightweight, high-strength prosthetic. The suggested design, which has a smooth roll-over shape and a good response to energy return requirements in ankle-foot prosthetics, proceeds as a non-prismatic cantilever beam with the design of the keel and heel. The FEA analysis showed that the vertical loading test successfully caused deflections in the heel and keel, and that the strain and stress in all three tests were within acceptable ranges. The energy was also stored and returned in the ankle-foot prosthesis. Song et al. [18] manufactured a new prosthetic foot design (laminate type with composite plates) to reduce cost without affecting walking comfort and flexion performance (The foot should be designed with a constant thickness curvature and in accordance with length). The materials are composite plate uses woven-type carbon fiber (WSN3 K) and unidirectional (UD) glass fiber (UGN200B). To enhance the bending properties on both sides, achieving highly equivalent toe and heel performance comparable to the LP Vari-Flex, prosthetic foot designs were developed using FEA with the ABAQUS software. Performance tests were conducted based on the KS P 8403 standard. The foot is made of a composite material with a uniform, bendable polyurethane rubber overlay. Due the foot easy to assembly the foot adapts to mass production and it low cost. The prosthetic foot demonstrates similar characteristics of bending in the toe and heel compared to the commercials Variflex foot. Womac et al. [19] studied how to measure the characteristics of the ESAR feet. The material is unknown. The modus operandi is to calculate the stiffness and energy storage of the prosthetic foot, the stiffness and heel wedge conditions, and force displacement data were collected in combinations of 15 sagittal directions and 5 coronal directions during the mechanical test used in this study. The conclusion is that stiffness class, manufacturer, orientation, and heel wedge are the factors affecting stiffness, energy storage, and return characteristics (in the sagittal and coronal planes, stiffness and associated energy storage are nonlinearly correlated). In all prosthetic foot types, energy storage increases with the anterior, medial, and lateral loading directions, while stiffness decreases with increasing heel, anterior, medial and lateral loading directions The effects of the heel wedge were affected by the prosthetic foot. Catto [20] studied how to run a dynamic simulation of the gait cycle stance phase; This study re-simulates the elastic behavior of a conventional commercial prosthetic foot using a multibody analysis. The material is carbon fiber. The methodology based on define stiffness' starting value and on order to realize a multibody model a segmentation was carried out for the prosthetic foot. Additionally, the Variflex foot's quasi-static loading simulation is regenerated utilizing the data obtained from quasi-static mechanical simulations to preserve the stiffness of the joints. In order to identify the mistakes made when calculating foot deflection and rollover Shape over gait, simulate gait effects on the multibody model. The conclusion: This study demonstrates that a multibody model can be used to successfully perform a dynamic analysis of the stance phase. Additionally, this type of simulation can be completed more quickly than a full finite element method (FEM). Additionally, the rollover shape radius of curvature can be calculated in less than 10 minutes with an error of less than 4%. To obtain the same values, a complete FEM could take longer than an hour. Tryggvason et al. [21] presented a case study on a prosthetic foot design that has undergone modifications to provide variable stiffness. Simulation A control damping element can be added and connected in parallel and in series with a system of springs as part of modifications made using finite element modeling and design change. The intention is to change the device's stiffness under approximate dynamic loading. The material is carbon fiber composite leaf springs. The methodology includes that; measuring the load response in a full rollover of the prosthetic foot, using FEA and dynamic modeling to simulate mechanical testing methods. The element's activation during the foot loaded is justified by the damping effect. It is crucial to calculate the dissipation energy in such an element because that is where the damping contrasts with the primary design objectives of Energy Return in the prosthetic foot. Our design case demonstrates that adding a damping element with a high damping constant can increase the machine's overall rotating force by 50%. The energy dissipation of the active element is approximately 20% of the maximum stress energy given a large enough grant damping coefficient. Kamel et al. [22] demonstrated an ingenious topology process in which improvements were successfully incorporated into the development of the prosthetic foot, and its function and cost-effectiveness reduced the effort expended while walking. The substance is PLA. The methodology is based on: (Create a design for a prosthetic foot model with basic dimensions / Next, apply structure technology to create a perfect visual model / Get help from a prosthetist to develop the model using experience / Build a FE model / Fabricate a prototype using 3D printing / Test Experimental model (test materials)). The bottom line includes the following: A direct spring has been specially created and produced to reduce the energy used during the gait cycle. This mechanism conserves approximately 70% the total energy of healthy subjects. Experimental tests were used to validate the model. In addition, a special adapter that was 3D printed for this process was used just to test the model. Their design is safe for patient use, due to the testing process. It was discovered that we can use PLA to create prostheses due to its light weight and good strength. Considering our 3D printed model cost just over $10 instead of SACH's $600 imprint, it was a lot less expensive. However, this synthetic model provides a mechanism for ESAR, which reduces metabolic energy during different levels of activity.

Ali [23] proved that all prosthetic foot designs today, even the most popular and widely used, do not replicated the contours of a natural foot. This research aims to identify an ideal design and construction of a prosthesis that provides similar characteristics to a healthy human foot, and the second goal is to combine these characteristics of a foot prosthesis to achieve a multifunctional prosthesis. The material used was polyethylene. The working method is to present the results of static and fatigue analysis in the analytical component using numerical methods FEM and experimental methods. The conclusion is a higher dorsiflexion angle, greater flexibility in the non-articulated foot when using a new high-density polyethylene design (by slotted area in the upper side), better stability and balance (by lengthening the keel), and a longer fatigue life, but the result shows the same effect of SACH feed absorb energy. The price per foot is 80% lower than comparable products, and it weighs 25% less. Maitland et al. [24] used FEA in computer simulations to investigate how the stiffness, width, and toe splitting of a prosthetic foot affect the ground foot's motion during the stance phase of walking on a cross-slope surface. The material is carbon fiber. The method relied on the construction of a foot model and simulations with ANSYS, with the following variables: cross-slope angle, foot stiffness, body mass, foot width, number of splits, lateral deviation in millimeters, vertical displacement in millimeters, forward pylon velocity, and foot contact. With increasing foot stiffness, there is a corresponding decrease in vertical displacement, mediolateral displacement, and forward velocity as well as an increase in cross slope. Conversely, with decreasing foot stiffness, there is a corresponding increase in foot contact, mediolateral displacement, and forward velocity on cross slopes. Wider foot designs resulted in more foot contact, but cross-slope intermediate displacement increased. Enhance and lessen foot contact when compared to full toe variations, lateral medial displacement using single and double toe designs results in two or three cantilever springs. Quraishi et al. [25] decoupled energy storage and return (DESR) foot, the prosthesis' mechanical PO energy can be increased by taking advantage of the wasted energy during the heel contact the ground and loading response. The material is unknown. The method of work includes that; describing the construction and characteristics of the DESR ankle prosthesis mechanism and evaluating its efficacy on a benchtop. This decoupling mechanism could also include the addition of other adjustments; this idea might be pursued in further research. The conclusion includes a dual cam-follower transmission was created using two nonlinear torque-angle curves to give the ankle mechanics a special degree of customizability. By creating a single model to separate the tracks of ESAR, this mechanism was presented. This mechanism was able to decouple the storage and return of energy, but it was unable to generate net-positive mechanical work for the PO. During PO, the DESR mechanism returned additional energy, but the amount was insufficient to completely offset the mechanical system's hysteresis losses.

Rajput et al. [26] created a prosthetic foot and calf to solving the traditional foot problems that include heavy weight, high price, and difficulty in manufacturing, the new design provides an approach that includes light weight, reduce the load, easy to doff and don and a hybrid optimization by using a topology optimization. The material is unknown. The method of work includes determine how much stress would be placed on the designed prosthetic, it was simulated walking. The methodology consists of the following steps: 3D scanning the leg; 3D scanning the leg model; preprocessing for generative design; analysis of the generative design outcomes; manual modifications to selected outcomes; weight reduction and surface lattice generation; design and analysis of a compliant foot; use of video recording for the foot; and calculation of the force and stress on the foot during walking using the ANSYS program. Do simulations for the foot after that to ensure that the component does not fail when the load is applied. The foot is constructed using SolidWorks ankle joints, and compliant joints have been used in place of the toe joints to create a one-piece design that is lighter and stronger while still operating similarly to a normal foot. Use an ANSYS program to calculate the force and stress on the foot while walking while using video recordings of the foot to study the gait cycle. Tabucol et al. [27] aimed to study and consider the loads and stresses to which the healthy human foot is subjected during the development of the energy-storing foot which was one of the factors that made it necessary to develop the foot into ESAR feet. The energy storage foot has been developed in terms of rigidity. Material: carbon fiber or fiberglass. The working method is to make improvements to the finite element structural analysis, ISO 10328 standard static test, and functional validation methodology. The conclusion is that a methodology based on finite element analysis and experimental techniques has been used to design the elastic components of the prosthetic feet and to investigate their functionality. This methodology can be used to create novel ESAR designs for a range of weight classes. The method used as a tool to search for new systems that could be integrated into existing ESAR feet to alter the stiffness/damping characteristics.

Hameed and Ali [28] designed, analyzed, and manufactured a foot model that energy storing and releasing (The type of heel is spring) used during the gait cycle for walking and running for above knee patient. The materials are carbon woven fiber and epoxy resin. The method of work includes that; Foot is created and assembled using SolidWorks, and analysis is done using ANSYS Static tests that are done in accordance with ISO 10328. According to Aircraft Owners & Pilots Association, foot thickness increased gradually until it reached the required specifications in the allowable strength limit. The conclusion includes that; the stress value in the heel and vertical load test may be similar to or the same as the maximum stress and maximum displacement in dorsiflexion when the keel is in contact with the ground. Although there is a linear relationship between load and displacement in the keel, the relationship is non-linear in the heel. Carbon fiber is preferred because it is a lightweight, strong material.

After reviewing the majority of the studies on the ESAR prosthetic foot, it was determined that all of the studies were focused on developing an ESAR prosthetic foot that is somewhat similar to the human foot in terms of the energy used to PO when walking and the movement of the ankle joint. The studies also focused on creating a stiff foot that does not break, bears human weight, and allows for faster walking on flat surfaces. Due to traditional feet's inability to produce a smooth walking pattern that is equal to the normal gait cycle in terms of ESAR, the amputee exerts greater weight on the healthy leg, which can lead to osteoarthritis in the knee joint of the unaffected side, exposing the knee to the disease. Some studies have focused on the need for the foot to have appropriate mechanical qualities for amputees engaging in moderate exercise. They have also concentrated on the foot's price and weight. Choosing the right materials for the foot and selecting the appropriate manufacturing process was also crucial. An optimal material that can support a person's weight and store and return energy during the PO phase of the gait cycle must be chosen, as must a design that plays a useful part in supplying this mechanism. The old traditional foot, the carbon foot, and the 3D-printed foot were all used in the investigation. For lower limb amputees, the foot is typically the most important part of the prosthesis, making the choice of foot type critical for the patient's comfort and ability to walk normally.

Today, ESAR feet are among the most crucial because they offer a gait pattern that relies on energy recovery and saving, preventing high energy expenditure during the gait cycle. Given the dearth of information and overlap in the literature on ESAR foot, studies are summarized in this study. As a result, the research was organized according to the goal, the type of material, the previous theory adopted, and the conclusion. This allowed the researcher to quickly review the research and its results as well as learn about the most popular materials currently in use, such as carbon fiber, as well as the successes and failures of other studies. This helps expediting a protracted research process.

3.Methods

A foot model made of ABS, previously studied and found to have structural weaknesses, was intended to be redesigned using CAD modifications [14]. The model was created in SolidWorks 2012 as a 3D sketch, using two-dimensional(2D) photographs to convert a 2D image to a 3D graphic, this includes inserting a side view image into the SolidWorks from the prior study as a reference. The foot model is recommended for women and young people with knee amputation, especially those with K3 activity level (the patient has the ability to ambulate (walk) with a varied rhythm (speed)). This foot was chosen for its ability to ensure smooth step coordination and adapt to varying walking speeds while providing propulsion energy. This reduces the effort required by the patient and allows seamless transitions through different phases of the walking cycle. Additionally, it demonstrates high efficiency in adapting to diverse surface types, which can often pose challenges for walking, ensuring stability and ease of movement. Model dimensions are (245×143×81) mm in length, height, and width order. Based on the measurements stated, the lines were drawn in the research and the side view image (245 mm long foot with a height of 143 mm and a breadth of 81 mm), as shown in *Figure1(a)*. The sketch was extruded, as indicated in *Figure1(b)*, with a width of 81mm and the pyramid adapter was extruded after drawn it, as seen in *Figure 1(c)*. The forefoot and foot width were cut in an oblique shape, as indicated in *Figure(d)*. A 2mm fillet along the foot's whole edge was created. Final shape of the foot was constructed, as shown in *Figure 2*.

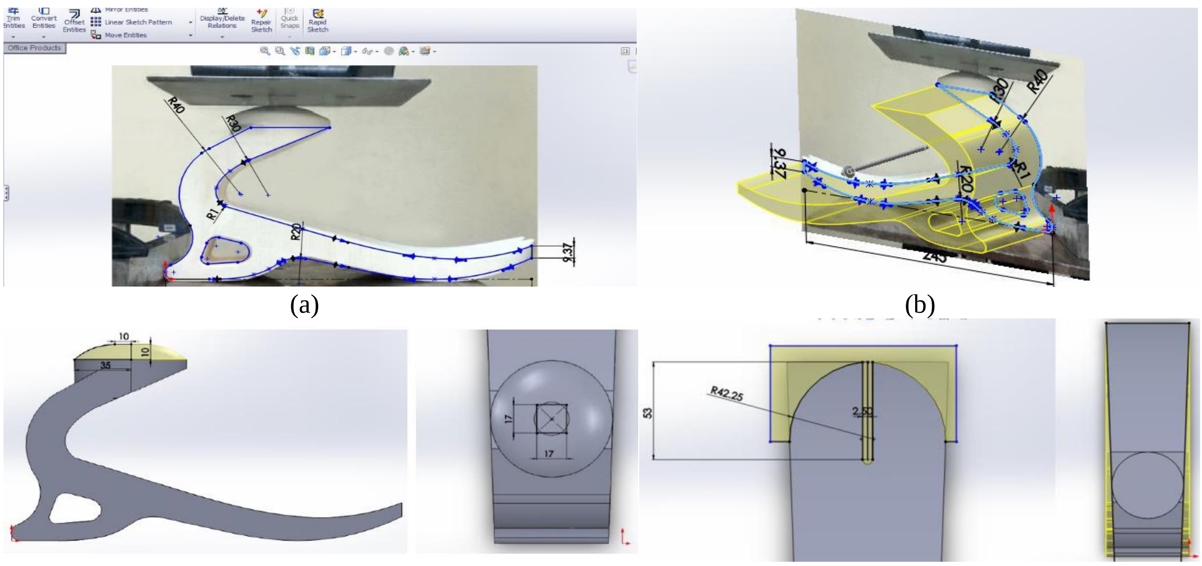

(a) (b)

(c) (d)

Figure 1 Steps to draw a foot model

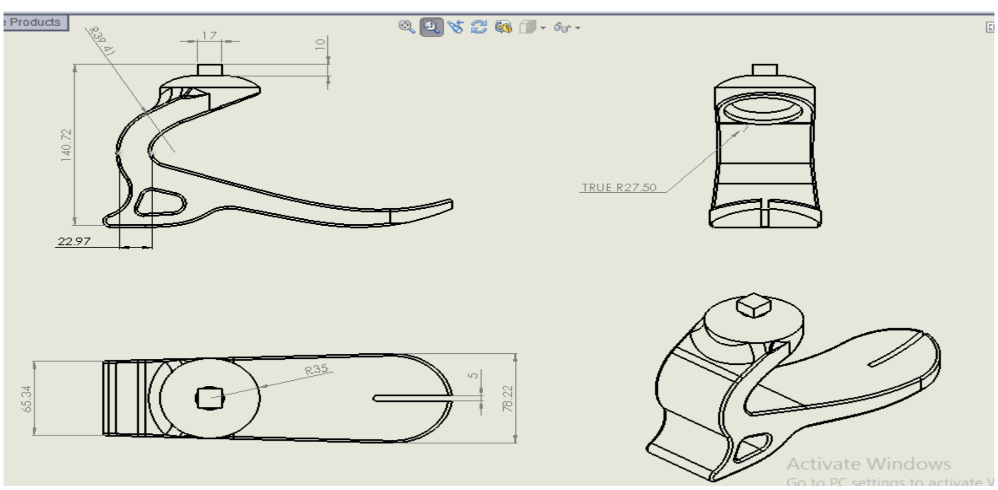

Figure 2 3D dimension of the foot model

To ensure the development process is conducted correctly, two theories are used. The first focuses on changing the materials used to construct the foot and identifying which materials have the ability to resist failure. This is achieved theoretically by conducting an engineering analysis for each foot made from a different material, determining the von Mises stress, safety factor, total deformation, and strain energy. The second theory is based on making changes to the foot design and conducting the same previous tests to find out which designs are the ideal design and also finding the safety factor in the dynamic state. The durability and comfort are directly proportional to the increase in the von-Mises stress and total deformation.

The first method involves changing the type of material using PLA carbon fiber once and PETG carbon fiber again. This method includes testing the foot model theoretically using the ANSYS program version 16 and SolidWorks version 12.

Export the foot model file from SolidWorks as an initial graphics exchange specification (IGES) file to ANSYS, and generate the model. Then, assign the mechanical properties of the material, specifically ABS Plus-Plai, as obtained from the previous study, as shown in *Table 1* [14].

Table 1 Mechanical properties of ABS material

Property	Value	Unit
Density	1.03	g/cm^3
Young's Modulus	2.2E+09	Pa
Poisson's Ratio	0.35	
Bulk Modulus	2.4444E+09	Pa
Shear Modulus	8.1481E+08	Pa
Tensile Yield Strength	3.1E+07	Pa
Tensile Ultimate Strength	3.1E+07	Pa

Then mesh generation (it is a network formed of cells and points (or nodes) distribution, smoothness, and skewness) for the foot model is the process of generating a 2D and 3D grid with an element size of 2 mm with slow translation between smooth edges (capabilities help reduce the amount of time and effort spent to get to accurate results), as shown in *Figure 3*.

The foot is then tested based on the gait cycle to theoretically analyze its behavior during all phases. This involves studying the loads it is expected to experience during each phase of the gait cycle, including heel strike (HS), when the heel touches the ground; mid-stance (MS), when the foot is in full contact with the ground; and push-off (PO), when the toes touch the ground, and the heel lifts off the ground, as described in the previous study [14].

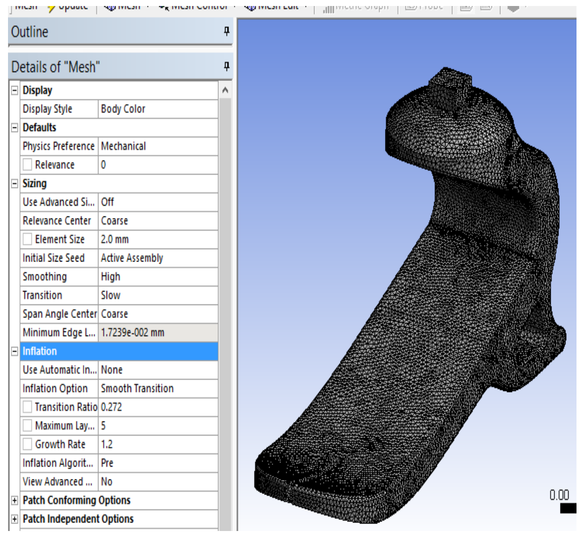

Figure 3 The details of mesh sizing and inflation

All boundary conditions were applied using the FEA (calculations, models, and simulations are used to predict and comprehend how an object might behave under various physical conditions). A person with a body mass of 60 kg was assumed to match the prototype's dimensions. The model's vertical load (900 Newtons) was 1.5 times the weight of the subject [29]. The simulation was conducted in a static state to calculate the von Mises stress, which is used to predict material yielding under complex loading conditions based on the results of uniaxial tensile tests [30]. The analysis began with the HS phase by fixing the heel of the foot model and applying a vertical load of 900 N to the ankle using the ANSYS program, as illustrated in *Figure 4*.

The simulation was repeated once for the midstance phase, by fixing the heel and the forefoot and placing the load vertically on the ankle, and then for the last stage of walking, which is the PO phase. This can be represented in two ways. In the first method, the forefoot is fixed, and the load is applied to the ankle. In the second method, the process is reversed: the ankle is fixed, and the load is applied to the forefoot from the underside of the foot. The fixation occurs during the HS phase and is subjected to two additional loads. The first is the lateral forces (LF) resulting from inversion and eversion movements, defined as 23% of the body weight, which corresponds to 207 N [29]. This process involves applying a load of 207 N to the ankle while fixing the heel. Additionally, an auxiliary torque (AT) of 15,750 N was applied. The torque was calculated by taking 23% of the body weight (900 N) and multiplying it by the lever arm distance between the ankle and the heel, approximately 7.6 mm. This setup consisted of applying a torque of 15,750 to the ankle and fixing the heel, as illustrated in *Figure 5.*

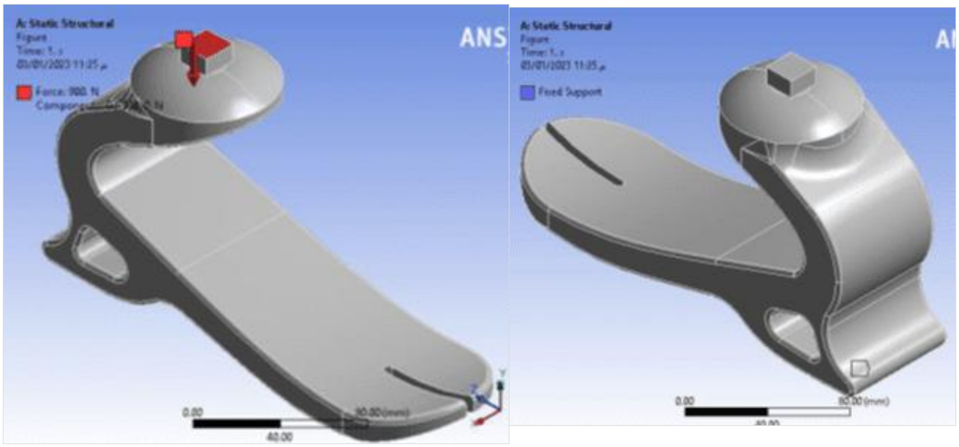

(a) (b)

Figure 4 Applying boundary condition for HS phase (a) Apply the force on the adapter (b) Fixation of the heel

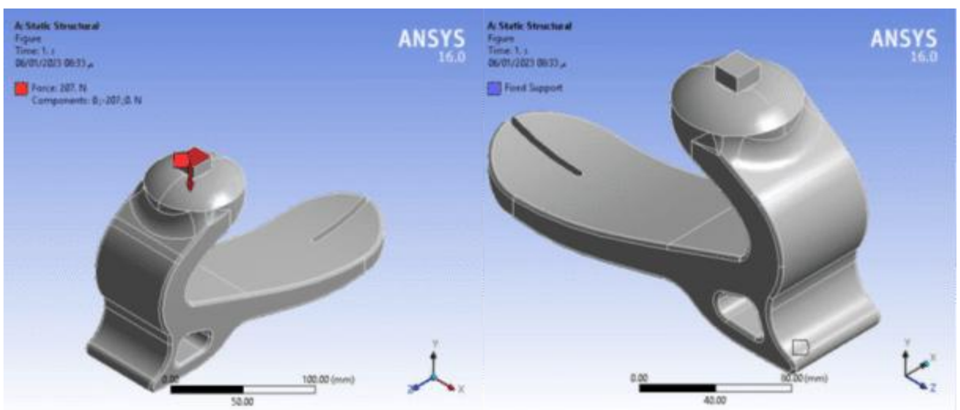

(a) (b)

Figure 5 Applying the boundary condition (a) Apply the torque on the adapter (b)Fixation of the heel

To ensure consistency in the design, the results of the previous study were compared with those of the current study using the percentage variance. This percentage measures the difference between the forecasted and actual results for von Mises stress. The percentage variance is calculated as the difference between two values, divided by the first value, and then multiplied by 100 [30]. Additional results were obtained in this research through theoretical calculations performed using the ANSYS program. These results include the total deformation (a measure of how much an object is stretched), the safety factor (the ratio between the material's yield stress and the maximum von Mises stress in the part, which indicates whether the design can withstand the applied loads without damage, bending, or breaking), and strain energy (a form of potential energy stored in materials subjected to strain). These parameters were not included in the previous study, as described in Equation 1 [30].

Factor of safety = Yield stress / Maximum von Misses (1)

The aim of extracting the total deformity is to determine the extent of deformation (the forward motion experienced by the ankle structure before returning to its initial position during the gait cycle). This deformation is directly proportional to the strain energy, which reflects the amount of energy stored within the structure. The safety factor plays a critical role in reducing the likelihood of product failure and increasing its overall reliability. It is particularly important in applications involving fall protection and safety gear, where failure can result in serious injury or death, as well as significant financial losses for the business. Ensuring an adequate safety factor helps mitigate these risks and enhances the product's dependability.

After verifying that the design aligns with the results from the previous study [14], the development phase begins. This phase involves repeating the previous steps for ABS but replacing the material first with PLA Carbon Fiber and then with PETG Carbon Fiber. These materials were selected for testing on the original foot model due to their wide availability in Iraq and their ranking among the top five carbon fiber filaments for 3D printing. Research has shown that combining continuous carbon fibers with polymers can enhance composite strength, rigidity, and thermal conductivity while simultaneously reducing part deflection, making these materials ideal for the study. In addition, these composites outperformed carbon fiber-reinforced polymer composites in terms of mechanical strength and performance. Due to their excellent mechanical qualities, recyclability, and potential for use in lightweight formulations, they are now replacing traditional metals as alternative materials [31–34].

PETG carbon fiber is a reinforced version of classic PETG filament, enhanced with carbon fiber to improve its mechanical properties and provide an attractive appearance. Compared to standard PETG, this material offers better dimensional stability, improved temperature resistance, a higher modulus of elasticity, and reduced stringing. However, it has slightly lower hardness than regular PETG. PETG carbon fiber produces durable, professional-looking prints suitable for outdoor applications.

Carbon fiber reinforced PLA, on the other hand, is a lightweight, strong material with excellent layer adhesion and minimal warpage. It provides high strength compared to other 3D printing materials and is characterized by increased rigidity. Unlike some other 3D printing materials, Carbon Fiber PLA is not necessarily "stronger" in terms of tensile strength but is much more rigid. This increased rigidity enhances structural support, though it reduces flexibility. Both materials are cost-effective and well-suited for applications requiring durability and stability [31–34].

Export the foot model design file from SolidWorks as an IGES file and import it into ANSYS. Generate a mesh with 2 mm element size, then assign the mechanical properties of the material—first for PLA carbon fiber and then for PETG carbon fiber—[32–33], as illustrated in *Figure 6*. Then all boundary conditions in the FEA design are applied as previously done in each of the three support stages (HS/MS/PO) in the static analysis.

Properties of Outline Row 4: CARBON FIBER PLA

	A	B	C	D	E
1	Property	Value	Unit		
2	Density	1.29	g cm^-3		
3	Isotropic Elasticity				
4	Derive from	Young's ...			
5	Young's Modulus	7665	MPa		
6	Poisson's Ratio	0.408			
7	Bulk Modulus	1.3886E+10	Pa		
8	Shear Modulus	2.7219E+09	Pa		
9	Field Variables				
13	Tensile Yield Strength	53.7	MPa		

(a)

Properties of Outline Row 5: CARBON FIBER PTEG

	A	B	C	D	E
1	Property	Value	Unit		
2	Density	1.34	g cm^-3		
3	Isotropic Elasticity				
4	Derive from	Young's M...			
5	Young's Modulus	2430	MPa		
6	Poisson's Ratio	0.442			
7	Bulk Modulus	6.9828E+09	Pa		
8	Shear Modulus	8.4258E+08	Pa		
9	Field Variables				
10	Temperature	Yes			
11	Shear Angle	No			
12	Degradation Factor	No			
13	Tensile Yield Strength	35.3	MPa		

(b)

Figure 6 Mechanical properties of a) PLA carbon fiber, b) PTEG carbon fiber

In addition to changing the material type, the foot underwent a second approach involving modifications to its design while maintaining the use of ABS Plus material. These design changes were compared to the original design to evaluate their effectiveness. As illustrated in *Figure 3*, several attempts were made to improve the foot design with the goals of reducing fracture risk, increasing flexibility, and enhancing energy storage. The design modifications focused on maintaining the basic structure while aiming to reduce stress on the keel's leaf spring.

Various strategies were explored, including adding a bumper to restrict the forward movement of the ankle during weight-bearing in the gait cycle and incorporating a spring-inspired S-shape to distribute pressure across multiple areas of the keel's leaf spring. The design changes were implemented iteratively, tested, and evaluated, with the optimal design selected based on the best results from von Mises stress analysis and the safety factor, as shown in *Figure 7*.

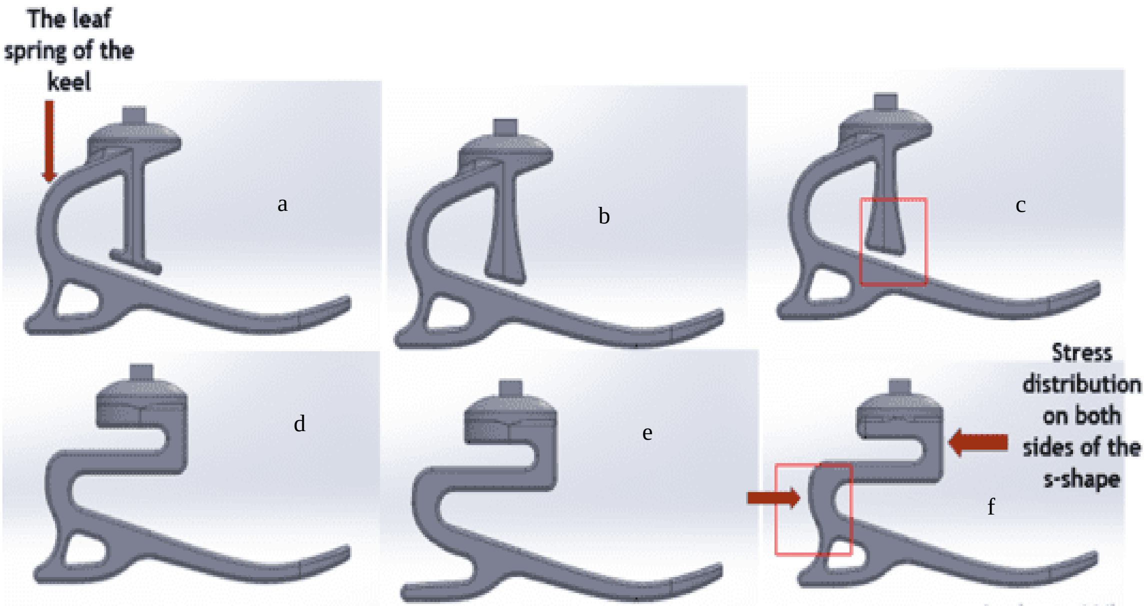

Figure 7 The suggested foot models

The design of the prosthetic foot was changed based on the results of the analysis. The adapter was placed in the last third of the foot, the ankle area was thickened, and an idea similar to a spring was made to transfer and distribute stress from the ankle area. This reduces fracture risk and increases energy storage in the prosthetic foot by generating torque arm between load and fixation points.

The modifications to the design include several key changes. In *Figure 7(a)*, a bumper was added to the ankle to measure strain in the foot and prevent the recurrence of a previous fracture. *Figure 7(b)* shows changes to the base of the bumper, which was exposed and had its sharp edges removed to improve its ability to withstand stresses. In *Figure 7(c)*, the end of the bumper surface was made parallel to the keel surface for better alignment. *Figure 7(d)* introduces an S-shape to the side connecting the bumper with the leaf spring, enhancing flexibility during the HS phase, distributing loads across multiple areas, and absorbing shock to reduce the risk of breakage. *Figure 7(e)* illustrates the removal of the heel support to improve shock absorption during the HS phase. Finally, *Figure 7(f)* depicts an increase in the thickness of the leaf spring to enhance its strength and reduce stress in the area where a previous fracture occurred.

After determining the optimal design by comparing the von Mises stress results and safety factors during the HS phase of the gait cycle, the selected model was compared to the original prosthetic foot from a previous study. This comparison involved simulating the ABS material properties theoretically using dynamic analysis in the ANSYS program. The safety factor was evaluated in the dynamic state for each phase of the gait cycle, with considerations for material degradation under repeated loading through fatigue simulation. Fatigue simulation, which is essential for assessing the life expectancy and durability of materials, components, or structures under cyclic loads, also ensures that safety criteria are met.

The fatigue properties of the ABS Plus material were derived from the S-N curve provided in a previous study. Mesh generation for the foot model was conducted by creating a 2D and 3D grid with an element size of 2 mm, utilizing slow translation and high smoothing, as shown in *Figure 8*. Boundary conditions included applying a force of 900 N to the upper part of the adapter, representing the ankle joint, and fixing the heel during the HS position. The stress applied was zero-based (repeated loading), as depicted in *Figures 9 and 10*, and the Gerber mean stress theory was used for the analysis, as shown in *Figure 11*. Details of the convergence process are illustrated in *Figure 12*.

Details of "Mesh"

Display	
Display Style	Body Color
Defaults	
Physics Preference	Mechanical
Relevance	0
Sizing	
Use Advanced Si...	Off
Relevance Center	Coarse
Element Size	2.0 mm
Initial Size Seed	Active Assembly
Smoothing	High
Transition	Slow
Span Angle Center	Coarse
Minimum Edge L...	5.1768e-002 mm
Inflation	
Use Automatic In...	None
Inflation Option	Smooth Transition
Transition Ratio	0.272
Maximum Lay...	5
Growth Rate	1.2
Inflation Algorit...	Pre
View Advanced ...	No

Figure 8 Mesh details

Details of "Fatigue Tool"

Materials	
Fatigue Strength Factor (Kf)	1.
Loading	
Type	Zero-Based
Scale Factor	1.
Definition	
Display Time	End Time
Options	
Analysis Type	Stress Life
Mean Stress Theory	Gerber
Stress Component	Equivalent (Von Mises)
Life Units	
Units Name	cycles
1 cycle is equal to	1. cycles

Figure 9 The details of fatigue stimulation

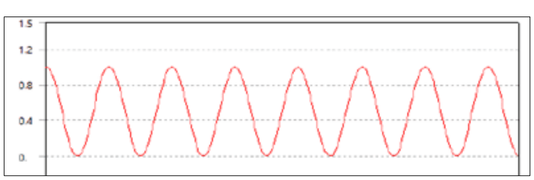

Figure 10 Constant amplitude load zero-based

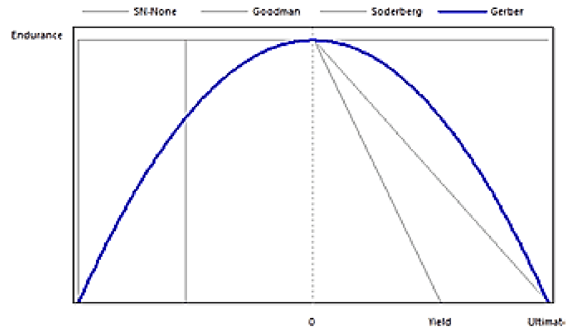

Figure 11 Mean stress correction theory

Details of "Convergence"

Definition	
Type	Minimum
Allowable Change	20. %
Results	
Last Change	-0.98908 %
Converged	Yes

Figure 12 Details of convergence

4.Results

A 3D image from the previous study [14], was obtained to further clarify the foot design, as shown in *Figure 13*. To advance the study and prevent fractures, the von Mises stress results of the original foot were compared with those of the foot modeled in this research. The percentage variation was then calculated to evaluate consistency with the foot analyzed in the previous study, as presented in *Tables 2*, *3*, and *4*.

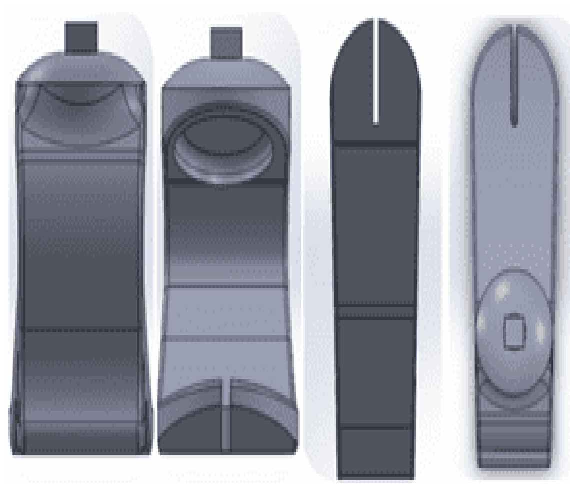

Figure 13 The foot design that has been chosen to developed it

Table 2 The simulation results of gait cycle's phases in previous study [14]

HS		MS	PO
Load (N)	900	900	900
Max stress of ankle (MPa)	11.562	11.562	11…37.799
Auxiliary torque at HS		LF at HS	HS total
Load (N)		207	*
Max stress of ankle (MPa)		2.6809	19.1684

All von Mises values in the *Table 4* are represented by the highest value of von Mises stress which is located in the ankle. Except for the first PO phase, where the highest stress does not occur in the ankle, the stress value in the ankle is taken, as mentioned in the previous study.

Table 3 The simulation results of this study

HS		MS	PO
Load (N)	900	900	900
Max stress of ankle (MPa)	11.74	11.73	10…36
Auxiliary torque at HS		LF at HS	HS total
Load (N)	15750	207	*
Max stress of ankle (MPa)	5	3	17

Table 4 The percentage of variation

Test phase	Percentage of variation %
HS	1.516
MS	1.516
PO first position	10
PO second position	4.759
HS with AT	1.49
HS with lateral force	10.636

The percentage difference was minimal, indicating that the model closely resembles the original design. Additional data were gathered to enable a more comprehensive study of the model, including calculations of total deformation and the safety factor for the original design. Further results, including total deformation, safety factor, and strain energy for the original design, are presented in *Figures 14* to *25*.

After analyzing the stresses applied during each phase of walking, the results indicate that the foot is capable of withstanding stresses during the HS and MS phases, as the safety factor exceeds 1.5. However, the highest total deformation occurs during the PO phase, rendering this phase unsafe, as the foot may be at risk of fracturing during walking due to a safety factor of 0.82 [36]. The results of this analysis are presented in *Table 5*.

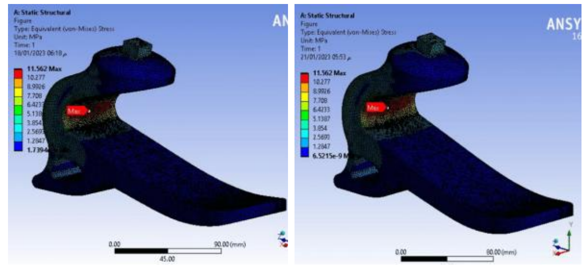

(a) (b)

Figure 14 Von mises stress for all phases for ABS plus (a) heel strike, (b) mid stance

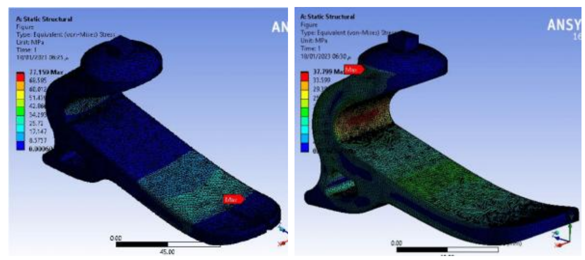

(a) (b)

Figure15 Von mises stress for all phases for ABS plus (a) first push off, (b) second push off

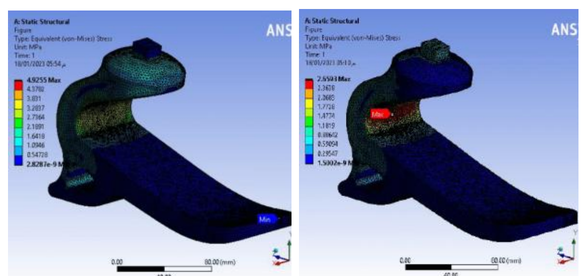

(a) (b)

Figure 16 Von mises stress for all phases for ABS plus (a) auxiliary torque, (b) lateral force

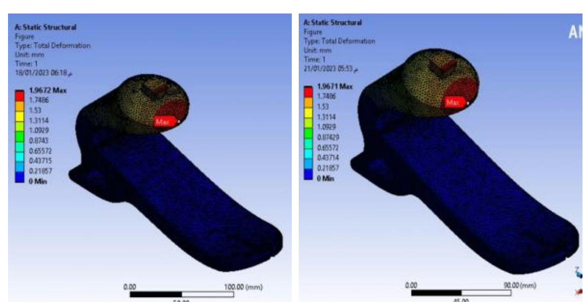

(a) (b)

Figure 17 Total deformation for all phases for ABS plus (a)heel strike, (b)mid stance

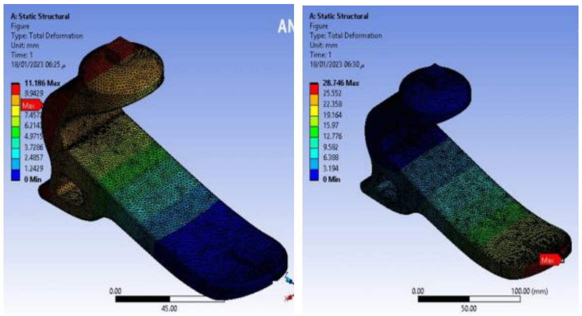

(a) (b)

Figure 18 Total deformation for all phases for ABS plus (a) first push off, (b) second push off

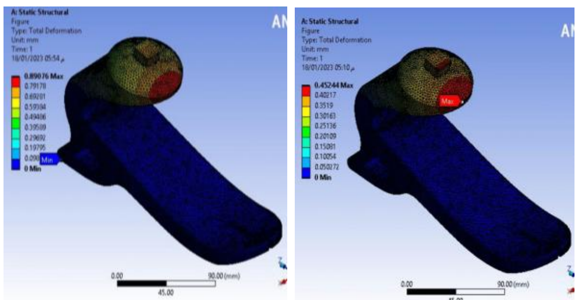

(a) (b)

Figure 19 Total deformation for all phases for ABS plus (a) auxiliary torque, (b) lateral force

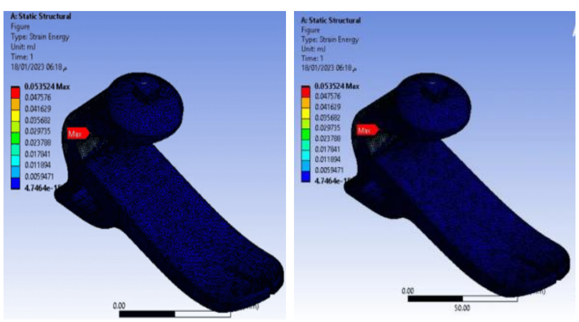

(a) (b)

Figure 20 Strain energy for all phases for ABS plus (a) heel strike, (b) mid stance

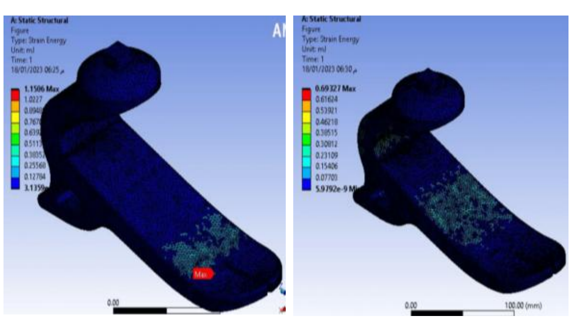

(a) (b)

Figure 21 Strain energy for all phases for ABS plus (a) first push off, (b) second push off

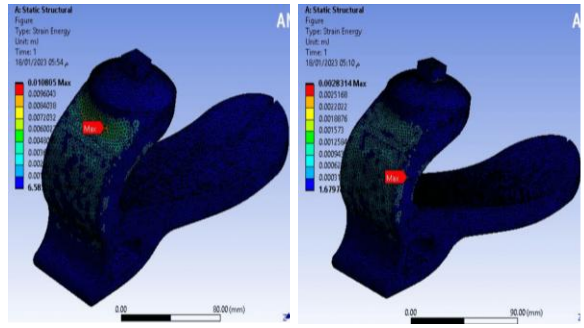

(a) (b)

Figure 22 Strain energy for all phases for ABS plus (a) auxiliary torque, (b) lateral force

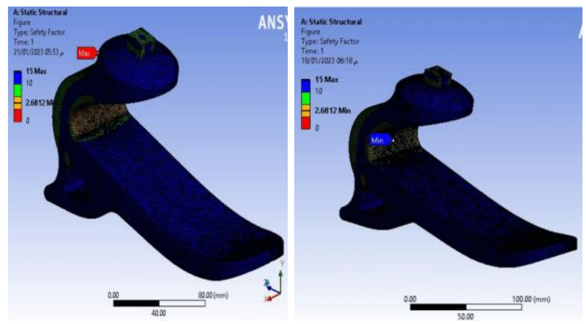

(a) (b)

Figure 23 Safety factor for all phases for ABS plus (a) heel strike, (b) mid stance

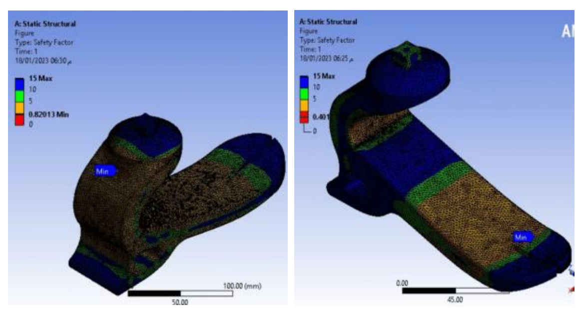

(a) (b)

Figure 24 Safety factor for all phases for ABS plus (a) first push off, (b) second push off

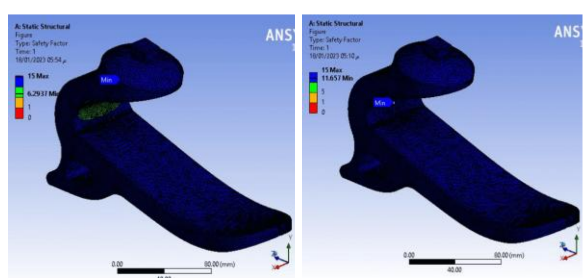

(a) (b)

Figure 25 Safety factor for all phases for ABS plus (a) auxiliary torque, (b) lateral force

Simulating the foot model after changing the material type involves reapplying the same stresses to represent the gait cycle. This simulation aims to determine the total deformation and safety factor for the original design. Obtaining results After a change in the material type of the foot (PLA carbon fiber and PETG carbon fiber), an analysis of the original foot model using FEA and the ANSYS workbench was performed, as shown in *Table 6*. The PO phase was simulated in two ways, and the second method was chosen because it simulates the natural movement of the foot during this stage. This was confirmed by imitating its movement with the ANSYS program and ensuring that the movement occurred in the ankle joint.

The results of the FEA analyses for carbon fiber PLA, carbon fiber PETG, and ABS Plus across all phases of the gait cycle were very similar in terms of von Mises stress during HS. The stress values were 11.562 MPa for ABS Plus, 11.723 MPa for carbon fiber PLA, and 11.843 MPa for carbon fiber PETG. Similar trends were observed for the other phases of the gait cycle. The safety factor also showed comparable results. For ABS Plus, the safety factor during HS was 2.6812, while for carbon fiber PETG it was slightly higher at 2.9806. Carbon fiber PLA showed a significant increase, with a value of 4.5808.

Regarding total deformation, carbon fiber PLA and PETG exhibited lower values compared to ABS Plus. During HS, the deformation in ABS Plus was 1.9671 mm, slightly reduced in carbon fiber PETG at 1.7445 mm, and significantly reduced in carbon fiber PLA at 0.55776 mm. This reduction in deformation resulted in decreased strain energy throughout the gait cycle. However, this behavior suggests that the foot may act as a structure that does not store and return energy effectively, which is essential for providing a natural and comfortable gait for amputees.

There is no significant difference observed when changing the material because most plastic materials exhibit similar behavior under loading conditions. However, the variations in results for total deformation and the safety factor are attributed to the intrinsic properties of the materials, such as strength, hardness, and stiffness. These material-specific characteristics influence how the foot model responds to applied stresses and deforms under load.

Table 5 The simulation results for all phases of gait cycle

Test phase	Von mises stress (MPa)	Total deformation(mm)	Strain energy (mm. J)	Safety factor
HS	11.562	1.967	0.053	2.681
MS	11.562	1.967	0.053	2.681
First PO	77.159	11.186	1.151	0.401
Second PO	37.799	28.746	0.693	0.820
AT at HS	4.925	0.891	0.011	6.294
LF at HS	2.659	0.452	0.002	11.657

Table 6 The simulation results for all phases for PLA and PETG carbon fiber for all phases of gait cycle

	Test phase	Von mises stress (MPa)	Total deformation (mm)	Stain energy (mm. J)	Safety factor
	HS	11.723	0.558	0.015	4.581
	MS	11.723	0.558	0.015	4.581
	First PO	73.592	3.149	0.306	0.729
PLA Carbon fiber	Second PO	38.381	8.143	0.194	1.399
	AT at HS	4.983	0.253	0.003	10.775
	LF at HS	2.696	0.128	0.001	15
	HS	11.843	1.745	0.046	2.981
	MS	11.843	1.745	0.046	2.981
	First PO	71.128	9.801	0.898	0.496
PETG Carbon fiber	Second PO	38.871	25.455	0.601	0.908
	AT at HS	5.026	0.794	0.009	7.024
	LF at HS	2.724	0.401	0.002	12.959

All models were analyzed, and the results for von Mises stress and the safety factor during the HS phase of each model were obtained. These results are presented in *Figures 26* and *27,* as well as in *Table 7.*

The F design was selected based on the analysis results because it demonstrated the lowest von Mises stress and the highest safety factor, as shown in *Figure 28*. The design modifications included repositioning the adapter to the last third of the foot, mirroring the structure of the human foot. Additionally, the ankle area was thickened to enhance strength, and an innovative S-shaped spring-like structure was incorporated. This feature helps to effectively transfer and distribute stress away from the ankle area, thereby reducing the likelihood of fractures and improving overall durability. After multiple design iterations, the final design was selected based on the analysis results, as presented in *Figure 29* and *Table 8*. The design modifications included repositioning the adapter to the last third of the foot, mimicking the structure of the human foot. Additionally, the ankle area of the prosthetic foot was thickened, and a spring-like shape was introduced to effectively transfer and distribute stress away from the ankle area. This innovation reduces the risk of fractures while enhancing the ESAR capabilities of the prosthetic foot. The design achieves this by generating a torque arm between the point of load application and the fixation point, thereby improving overall performance and durability. A fatigue simulation was conducted using the S-N curve values of ABS Plus material, obtained from the previous study [14], and applied to the design of the prosthetic foot model in ANSYS. This simulation was performed for both the original design from the previous study and the developed design, as illustrated in *Figures 1* and *24*. The results of the safety factor from the fatigue simulation are presented in *Table 9*. After confirming that the developed model produced satisfactory results in the static analysis, a dynamic (fatigue) simulation was performed to compare the safety factors of the original and developed models. The comparison revealed that both designs were deemed unsafe under dynamic conditions, indicating that neither model could endure a significant number of walking cycles without failure. These findings highlight the need for further improvements to enhance the fatigue resistance of the prosthetic foot.

The second method was an attempt to change the foot design with ABS Plus material. Many feet have been designed and tested in an effort to avoid the flaws of the old design, avoid a fracture, and try to reduce pressure on the leaf spring of the keel. The ideal design, which reduces breakage and provides energy storage was chosen after testing the model in ANSYS software using static analysis.

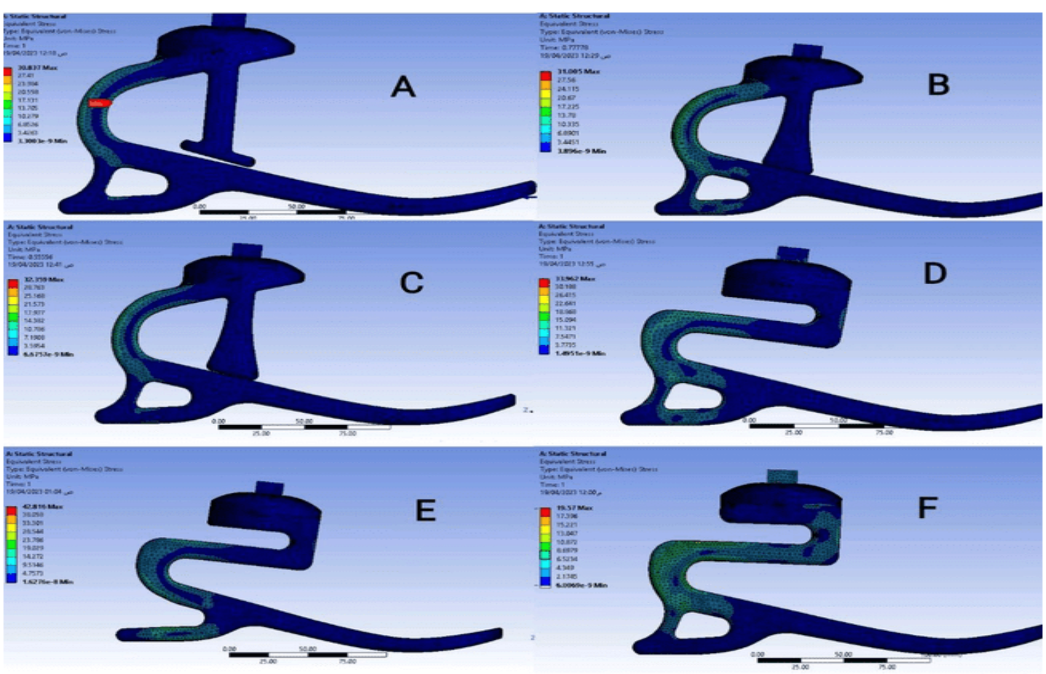

Figure 26 The result of von Misses stress for all designs

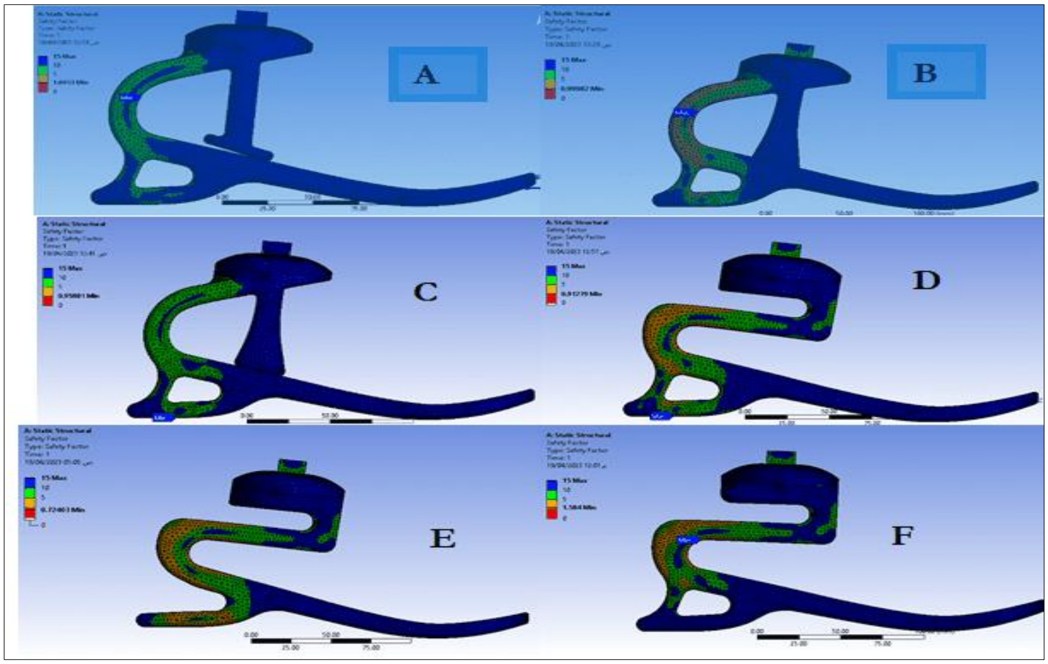

Figure 27 The result of safety factor for all designs

Table 7 The simulation results of developed foot designs (a), (b), (c), (d), (e), (f)

The figure	Von mises stress (MPa)	Safety factor
a	30.837	1.005
b	31.005	0.999
c	32.359	0.958
d	33.962	0.913
e	42.816	0.724
f	19.57	1.584

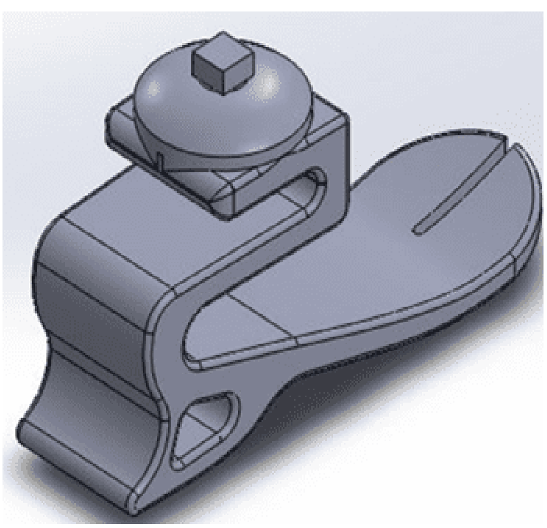

Figure 28 Developed foot design that has been chosen

The HS phase for the latest design, F, showed the best results compared to other designs. A change in the readings was observed, with total deformation increasing from the original design to a value of 4.7254 mm, the safety factor rising to 1.584, and von Mises stress increasing to 19.57 MPa. However, the designs were deemed unsuccessful due to high stress levels, reaching up to 42.816 MPa in the E design, and a safety factor below the standard threshold of 1.5, indicating that the designs were unsafe.

Subsequently, the original and advanced models were tested using dynamic analysis (fatigue simulation) to evaluate the foot's ability to bear the patient's weight and the various stresses encountered during the gait cycle. The results were unsatisfactory, with safety factor values significantly below the standard threshold of 1.5, ranging from 1.383e-6 to 8.183e-7. This indicates a 100% likelihood of the foot failing, even though the static analysis showed promising results. Such a structure poses a significant risk to the amputee, as it may result in the foot breaking and causing the user to fall, as illustrated in *Figure 30.* The convergence result of dynamic fatigue stimulation showed that there is no big different between before and after the convergence procedure and design life is 1. e+009 cycles and this indicates that the foot cannot withstand walking cycles and may break at any moment. as shown in *Figure 31*.

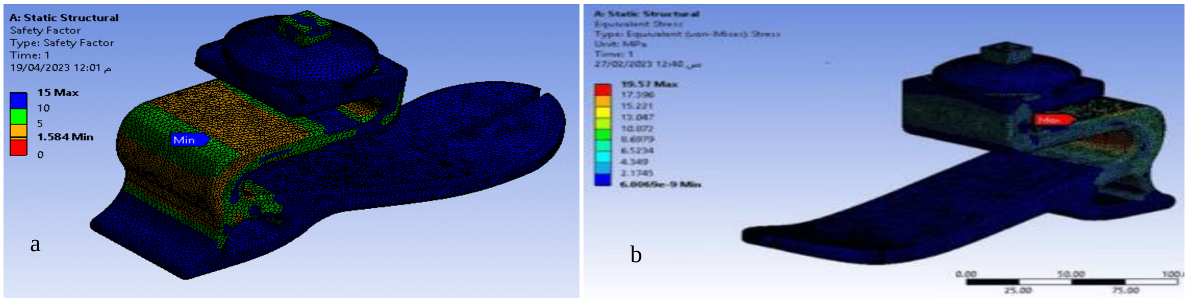

Figure 29 Heel strike a) safety factor, b) equivalent stress

Table 8 The simulation results of developed foot design of ABS material for all phases of gait cycle

Test phase	Von mises stress (MPa)	Total deformation (mm)	Stain energy (mm. J)	Safety factor
HS	19.57	4.725	0.186	1.584
MS	19.57	4.725	0.186	1.58
First PO	14.936	21.179	2.410	0.346
Second PO	64.254	75.397	2.062	0.482
Aux. T at HS	4.829	0.466	0.008	6.419
LF at HS	4.501	1.087	0.010	6.887

Table 9 The safety factor of fatigue stimulation for all phases of gait cycle

Test phase	The safety factor for original design in the previous study	The safety factor for design that was developed
HS	1.383e-6	8.183e-7
MS	1.383e-6	8.183e-7
First PO	2.075e-7	1.786e-7
Second PO	4.231e-7	2.491e-7
Aux. T. at HS	3.245e-6	3.311e-6
LF at HS	6.015e-6	3.554e-6

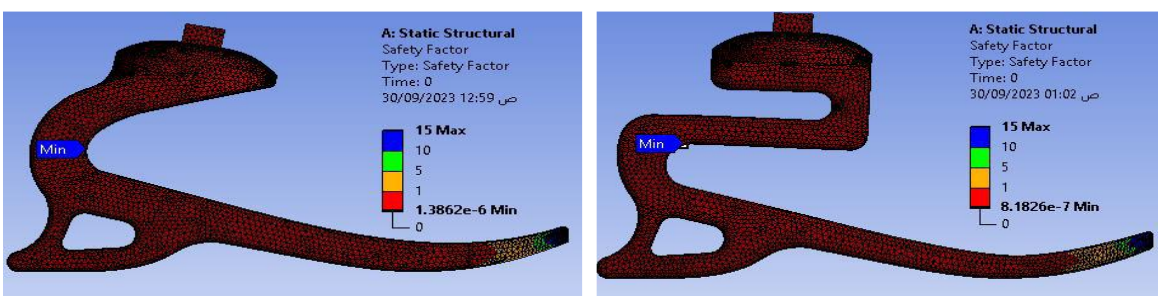

(a) (b)

Figure 30 The safety factor for a) original foot design, b) F design that was developed

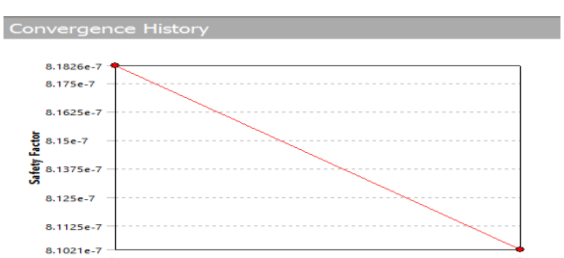

Figure 31 The convergence history

5.Discussion

Recent years have seen a rise in advancements in prosthetic foot technology, including changes in the materials and foot shape. Several studies have been carried out, with the primary goal being to develop a strong prosthetic foot that can store and return energy. An attempt to use AM techniques, specifically a 3D printer, to build a prosthetic foot is among the most current experiments. A particular kind of composite material, such plastic or polymer, is needed for this process. ABS, nylon, PLA, PETG carbon fiber, and other plastic compounds are currently accessible in Iraq. A broken ABS plus foot model was chosen for theoretical development in this study utilizing ANSYS 2016 and SolidWorks 2012. Initially, the original foot model was recreated based on a 2D image using the SolidWorks program. This 3D model was then tested using the ANSYS program, and the results were compared to the original research data to verify the accuracy of the recreated model. The comparison revealed that the variation in stress values across all phases of the gait cycle was minimal, ranging from 1.5% to 10.6%, confirming that the 3D model closely resembled the original design.

This effort aimed to develop a foot model using two distinct methods. Since ABS is a stiffer material than elastic, an effort was made to switch up the material type in the first approach. PLA and PETG carbon fibers are the most readily available materials used in 3D printing in Iraq and have been shown to be successful; they were selected for testing because they combine flexibility and hardness. The findings were FEA evaluations of ABS, PETG, and PLA carbon fibers for every gait cycle. Very similar in terms of von Mises stress; in HS for ABS Plus, the stress value is 11.562 MPa, for 11.723 MPa for carbon fiber PLA, and for 11.843 MPa for carbon fiber PETG, and so on for the rest of the phases. The safety factor showed similarity in the results between ABS Plus with a value of 2.6812 in HS and for carbon fiber PETG with a value of 2.9806 and an increase in carbon fiber PLA with a value of 4.5808. However, total deformation was lower in carbon fiber PLA and PETG than in ABS plus, with the HS in ABS plus measuring 1.9671 mm, a slight decrease in carbon fiber PETG measuring 1.7445 mm, and a significant decrease in carbon fiber PLA measuring 0.55776 mm. This resulted in a decrease in stress energy throughout the gait cycle, meaning that the foot acts as a solid body without storing and returning energy, which is required to provide amputees with a natural and comfortable gait. There is no significant difference when changing the material because most plastic materials are similar in their behavior. In the second method, an attempt was made to change the foot design with ABS Plus material. Many feet have been designed and tested in an effort to avoid the flaws of the old design, avoid a fracture, and try to reduce pressure on the leaf spring of the keel. The ideal design, which reduces breakage and provides energy storage, was chosen after testing the model in ANSYS software using static analysis. The HS test for the latest design, F, showed the best results compared to other designs, and we noticed a change in the readings, as the total deformation increased from the original design at a value of 4.7254 mm. Strain energy also increased to 0.1863 mJ, with a safety factor with a value of 1.584 and a von Mises stress of 19.57 MPa, while the rest of the designs were not successful due to exposure to high stress up to 42.816 in the E design, and the safety factor is less than the standard ratio of 1.5, meaning that the designs are not safe. Subsequently, the original and advanced models were tested with dynamic analysis (fatigue stimulation) to find out the extent of the foot's ability to bear the weight of the patient and all kinds of stress that were tested during the gait cycle, and the results were unsatisfactory; that is, the safety factor is much less than the fixed standard ratio of 1.5, as their value ranged between (1.383e-6 to 8.183e-7), indicating that the foot will break 100% even if it shows good results. In the static analysis, this structure poses a risk of the foot breaking and causing the amputee to fall [37]. After conducting previous tests on several models of designs and different materials used to manufacture the foot, with the aim of increasing the efficiency of the foot in terms of safety and stored energy, it was concluded that these designs and models were not safe to use and were not able to withstand stresses while walking, regardless of the amount and quantity of energy that they could store. This indicates that the materials used in 3D printing may not be able to bear the weight of a person and the stresses placed on the foot during walking. Therefore, it is possible for any plastic material from 3D printing to break. It is possible in the future to make composite materials with plastic to strengthen it and change its mechanical properties and make it bear different stresses during the walking cycle. A complete list of abbreviations is listed in *Appendix I*.

6.Conclusion and future work

All advancements and efforts to develop new prosthetic feet aim to create models that are easy to manufacture, lightweight, and completely safe for amputees. One of the key factors influencing the success of a prosthetic foot is the material's properties, including strength, rigidity, and flexibility. These attributes are essential for ensuring that the foot allows the patient to walk naturally and safely. Equally important is the design of the foot, which should resemble a healthy human foot and enable natural movement for the body. This study found that while changing the material, particularly among polymer-based materials such as ABS Plus, PETG carbon fiber, and PLA carbon fiber, can have some impact, it was not the primary or most effective factor in improving the foot's performance. In contrast, changes to the design had a more significant effect, with results varying depending on the specific design. It is also important to note that plastic materials lack the capacity to provide optimal foot functionality due to their susceptibility to fractures during the walking cycle, as demonstrated in the fatigue simulation results. This is primarily due to the repeated stresses they endure. In the future, advancements in polymer technology may potentially address this limitation by creating composite materials with higher efficiency. Alternatively, hybrid designs could be explored, such as using different materials for different parts of the foot—for example, constructing the heel from one material and the rest of the foot from another, or incorporating a rubber-like material within the foot to absorb shocks. Despite these possibilities, the fundamental issue remains that plastic materials generally do not resist fatigue well and are prone to breakage. However, current research continues to support the effectiveness of carbon fiber due to its lightweight, durability, and ability to store and return energy. Therefore, it is recommended that future studies focus on developing prosthetic foot models using carbon fiber, as it holds great promise for addressing many of the challenges faced in current designs.

Acknowledgment

None.

Conflicts of interest

The authors have no conflicts of interest to declare.

Data availability

The data are not publicly available. However, the data may be provided by the corresponding author upon reasonable request.

Author's contribution statement

Noor B. Mohammed: Conceptualization, investigation, data collection, writing – review and editing. **Yassr Y. Kahtan:** Examine and correct the manuscript, supervision, Writing – review and editing.

References

[1] Pană CF, Manta LF, Vladu IC, Cismaru ȘI, Petcu FL, Cojocaru D, et al. The design of a smart lower-limb prosthesis supporting people with transtibial amputation-a data acquisition system. Applied Sciences. 2022; 12(13):1-18.

[2] Kim J, Wensman J, Colabianchi N, Gates DH. The influence of powered prostheses on user perspectives, metabolics, and activity: a randomized crossover trial. Journal of Neuroengineering and Rehabilitation. 2021; 18:1-3.

[3] Houdijk H, Wezenberg D, Hak L, Cutti AG. Energy storing and return prosthetic feet improve step length symmetry while preserving margins of stability in persons with transtibial amputation. Journal of Neuro Engineering and Rehabilitation. 2018; 15:1-8.

[4] Ehara Y, Beppu M, Nomura S, Kunimi Y, Takahashi S. Energy storing property of so-called energy-storing prosthetic feet. Archives of Physical Medicine and Rehabilitation. 1993; 74(1):68-72.

[5] Park JW, Greenspan B, Tabb T, Gallo E, Danielescu A. 3D printed energy return elements for upper limb sports prosthetics. Prosthesis. 2023; 5(1):13-34.

[6] Bowen J, Hausselle J, Gonzalez R. A low-cost customizable prosthetic foot with energy return capabilities. Prosthetics and Orthotics Open Journal. 2018; 2(1).

[7] Childers WL, Takahashi KZ. Increasing prosthetic foot energy return affects whole-body mechanics during walking on level ground and slopes. Scientific Reports. 2018; 8(1):1-12.

[8] Tuteski O, Kočov A. The application of additive manufacturing in developing 3D printed prostethics and orthotic devices. Industry 4.0. 2020; 5(1):23-6.

[9] Faustini MC, Neptune RR, Crawford RH, Stanhope SJ. Manufacture of passive dynamic ankle–foot orthoses using selective laser sintering. IEEE Transactions on Biomedical Engineering. 2008; 55(2):784-90.

[10] Gibson KS, Woodburn J, Porter D, Telfer S. Functionally optimized orthoses for early rheumatoid arthritis foot disease: a study of mechanisms and patient experience. Arthritis Care & Research. 2014; 66(10):1456-64.

[11] Kucewicz M, Baranowski P, Małachowski J, Popławski A, Płatek P. Modelling, and characterization of 3D printed cellular structures. Materials & Design. 2018; 142:177-89.

[12] Tack P, Victor J, Gemmel P, Annemans L. 3D-printing techniques in a medical setting: a systematic literature review. Biomedical Engineering Online. 2016; 15:1-21.

[13] Tao Z, Ahn HJ, Lian C, Lee KH, Lee CH. Design and optimization of prosthetic foot by using polylactic acid 3D printing. Journal of Mechanical Science and Technology. 2017; 31:2393-8.

[14] Rochlitz B, Pammer D. Design and analysis of 3D printable foot prosthesis. Periodica Polytechnica Mechanical Engineering. 2017; 61(4):282-7.

[15] Segal AD, Zelik KE, Klute GK, Morgenroth DC, Hahn ME, Orendurff MS, et al. The effects of a controlled energy storage and return prototype prosthetic foot on transtibial amputee ambulation. Human Movement Science. 2012; 31(4):918-31.

[16] Ray SF, Wurdeman SR, Takahashi KZ. Prosthetic energy return during walking increases after 3 weeks of adaptation to a new device. Journal of Neuroengineering and Rehabilitation. 2018; 15:1-8.

[17] Hamzah M, Gatta A. Design of a novel carbon-fiber ankle-foot prosthetic using finite element modeling. In conference series: materials science and engineering 2018 (pp. 1-15). IOP Publishing.
[18] Song Y, Choi S, Kim S, Roh J, Park J, Park SH, et al. Performance test for laminated-type prosthetic foot with composite plates. International Journal of Precision Engineering and Manufacturing. 2019; 20:1777-86.
[19] Womac ND, Neptune RR, Klute GK. Stiffness and energy storage characteristics of energy storage and return prosthetic feet. Prosthetics and Orthotics International. 2019; 43(3):266-75.
[20] Catto E. Realization and evaluation of a prosthetic foot multibody model in quasi-static and dynamic conditions. Doctoral Dissertation, Politecnico Di Torino. 2019.
[21] Tryggvason H, Starker F, Lecomte C, Jonsdottir F. Use of dynamic FEA for design modification and energy analysis of a variable stiffness prosthetic foot. Applied Sciences. 2020; 10(2):1-12.
[22] Kamel H, Harraz O, Azab K, Attia T. Developing an optimized low-cost transtibial energy storage and release prosthetic foot using three-dimensional printing. Journal of Engineering and Science in Medical Diagnostics and Therapy. 2020; 3(2):021103.
[23] Ali MM. Design and analysis of a non-articulated prosthetic foot for people of special needs. Doctoral Dissertation, Thesis in Mechanical Engineering. AL-Nahrain University. 2010.
[24] Maitland ME, Allyn KJ, Ficanha E, Colvin JM, Wernke MM. Finite element simulation of prosthetic foot adaptation to mediolateral-angled cross-slopes. JPO: Journal of Prosthetics and Orthotics. 2020; 32(4):236-44.
[25] Quraishi HA, Shepherd MK, Mcmanus L, Harlaar J, Plettenburg DH, Rouse EJ. A passive mechanism for decoupling energy storage and return in ankle–foot prostheses: a case study in recycling collision energy. Wearable Technologies. 2021; 2:1-13.
[26] Rajput S, Burde H, Singh US, Kajaria H, Bhagchandani RK. Optimization of prosthetic leg using generative design and compliant mechanism. Materials Today: Proceedings. 2021; 46:8708-15.
[27] Tabucol J, Brugo TM, Povolo M, Leopaldi M, Oddsson M, Carloni R, et al. Structural fea-based design and functionality verification methodology of energy-storing-and-releasing prosthetic feet. Applied Sciences. 2021; 12(1):1-26.
[28] Hameed MI, Ali AA. Finite element design and manufacturing of a woven carbon fiber prosthetic foot. Association of Arab Universities Journal of Engineering Sciences. 2022; 29(2):9-18.
[29] Major MJ, Twiste M, Kenney LP, Howard D. Amputee independent prosthesis properties-a new model for description and measurement. Journal of Biomechanics. 2011; 44(14):2572-5.
[30] Budynas RG, Nisbett JK. Shigley's mechanical engineering design. New York: McGraw-Hill; 2015.
[31] Yu T, Zhang Z, Song S, Bai Y, Wu D. Tensile and flexural behaviors of additively manufactured continuous carbon fiber-reinforced polymer composites. Composite Structures. 2019; 225:111147.
[32] Ferreira RT, Amatte IC, Dutra TA, Bürger D. Experimental characterization and micrography of 3D printed PLA and PLA reinforced with short carbon fibers. Composites Part B: Engineering. 2017; 124:88-100.
[33] Kannan S, Ramamoorthy M, Sudhagar E, Gunji B. Mechanical characterization and vibrational analysis of 3D printed PETG and PETG reinforced with short carbon fiber. In AIP conference proceedings 2020. AIP Publishing.
[34] Kabir SF, Mathur K, Seyam AF. A critical review on 3D printed continuous fiber-reinforced composites: history, mechanism, materials and properties. Composite Structures. 2020; 232:111476.
[35] Padzi MM, Bazin MM, Muhamad WM. Fatigue characteristics of 3D printed acrylonitrile butadiene styrene (ABS). In conference series: materials science and engineering 2017 (pp. 1-6). IOP Publishing.
[36] Kadry S, El HA. Numerical methods for reliability and safety assessment. Springer; 2015.
[37] Mohammed NB, Kahtan YY. Development, analysis and manufacture of a prosthetic carbon fiber foot model. In conference proceedings 2024. AIP Publishing.

Noor B. Mohammed, born on December 16, 1998, in Iraq, holds a B.Sc. and M.Sc. in Prosthetics and Orthotics Engineering. She is an experienced engineer with a strong background in designing and fabricating custom medical devices. Noor has a proven ability to collaborate effectively with healthcare professionals to develop innovative solutions that address the specific needs of patients, demonstrating her dedication to improving their quality of life.
Email: madehope1998@gmail.com

Yassr Y. Kahtan was born in Baghdad, Iraq, in March 1981. He earned his B.Sc. in Mechanical Engineering from Al-Nahrain University in 2002, followed by an M.Sc. from the same university in 2005. He completed his Ph.D. in Applied Mechanics at the University of Technology, Baghdad, in 2014. Throughout his academic journey, he received all degrees in Baghdad, Iraq. He is a former member of the International Society for Prosthetics and Orthotics (ISPO) and a consultant member of the Iraqi Engineers Association. Currently, he serves as an Assistant Professor in the Department of Prosthetics and Orthotics Engineering at the College of Engineering, Al-Nahrain University.
Email: yasir.yaarb@nahrainuniv.edu.iq

Appendix I

S. No.	Abbreviation	Description
1	2D	Two-Dimensional
2	3D	Three-Dimensional
3	ABS	Acrylonitrile Butadiene Styrene
4	AM	Additive Manufacturing
5	AT	Auxiliary Torque
6	CAD	Computer-Aided Design
7	DESR	Decoupled Energy storage and Return
8	ESAR	Energy Storage and Return
9	FDM	Fused Deposition Modelling
10	FEA	Finite Element Analysis
11	FEM	Finite Element Method
12	HS	Heel Strike
13	IGES	Initial Graphics Exchange Specification
14	LF	Lateral Forces
15	MS	Mid-Stance
16	PC-ABS	Polycarbonate/Acrylonitrile Butadiene Styrene
17	PETG	Polyethylene Terephthalate Glycol
18	PLA	Polylactic Acid
19	PO	Push Off
20	SACH	Stiff Heel Cushioned Ankle